Zeitschrift für Physikalische Chemie, **214**, 5, 675−703 (2000)

How do Parity Violating Weak Nuclear Interactions Influence Rovibrational Frequencies in Chiral Molecules?

By Martin Quack* and Jürgen Stohner

Laboratorium für Physikalische Chemie, ETH Zürich (Zentrum), CH-8092 Zürich, Switzerland

Dedicated to Prof. Dr. Dr. h. c. mult. H. Gg. Wagner on the occasion of his 70th birthday

(Received February 4, 2000; accepted February 10, 2000)

Infrared Spectroscopy / Chiral Molecules / Parity Violation / Electroweak Quantum Chemistry / Vibrational Spectra / Rotational Spectra

We outline the general theory as well as various approximations to the accurate calculation of vibrational and rotational transition frequency shifts between enantiomers of chiral molecules due to the parity violating weak nuclear interaction. The calculation of the effective parity violating potentials as a function of molecular geometry is mainly based on our recent, accurate Multiconfiguration-Linear Response approach (MC-LR, RPA and CASSCF, Berger and Quack, J. Chem. Phys. **112** (2000) 3148), which has been shown to lead to order of magnitude increases compared to early Restricted Hartree Fock (RHF) approaches. We present in some detail both the harmonic and diagonal anharmonic approach to parity violating vibrational frequency shifts. In these approaches the parity violating potentials are calculated as a function of all vibrational reduced normal coordinates q_i with the relevant matrix elements beeing obtained from harmonic and anharmonic vibrational wavefunctions. We also compare the adiabatic and reverse adiabatic harmonic approximation. In addition to the general exact theory several approximate approaches are introduced for the calculation of parity violating structural differences between enantiomers resulting in the corresponding changes of rotational transition frequencies. Results are presented for the chiral molecule CHBrClF. The predicted relative vibrational frequency shifts $\Delta_{pv}\omega_i/\omega_i$ are shown to depend strongly on the vibrational mode and the level of calculation (RHF, RPA, CASSCF) but in all cases are on the order of $10^{-(16\pm1)}$, much smaller than all previous experimental tests could detect. The predicted relative rotational frequency shifts fall in a similar range. We discuss consequences of our predictions for various possible experiments on molecular parity violation.

* Corresponding author. E-mail: quack@ir.phys.chem.ethz.ch

1. Introduction

Parity violation in nuclear physics was established in 1957 [1, 2] and the history as well as the unified electroweak theory [3−5] has been reviewed occasionally [6, 7]. Also, the consequences of parity violation in atomic physics and spectroscopy have been explored and reviewed [8, 9]. However, perhaps the most interesting consequence results in molecular physics, where parity violation leads to energy differences $\Delta_{pv}E$ between the left and right handed enantiomers of chiral molecules. From early on, the possible relationship of this energy difference and the preferred selection of L-aminoacids and D-sugars has been discussed [10−16]. Possible experiments for a measurement of $\Delta_{pv}E$ have been proposed [17] and these aspects have been reviewed [16], including extension to more general fundamental symmetry violations in molecular physics [18].

From the theoretical side an important development was the introduction of quantitative calculations of $\Delta_{pv}E$ based on quantum chemical techniques and perturbation theory [19−26]. There has recently been a renewed interest in improving upon these early calculations based on a Single Determinant Excitation-Restricted Hartree Fock (SDE-RHF) framework because of the discovery [27, 28] of an order of magnitude increase in $\Delta_{pv}E$, when going to a Configuration Interaction Singles excitation (CIS-RHF) approach, which has been reconfirmed more recently by independent computational techniques [29−33]. This discovery not only sheds new light on possible theoretical approaches but also is stimulating for developing experimental tests of molecular parity violation, which may be more easily detected than previously anticipated on the basis of the older results.

While a measurement of the parity violating energy difference $\Delta_{pv}E$ between enantiomers would be the most significant test of parity violation in molecules [17], one may conceive also other experiments. One possibility consists in demonstrating frequency shifts $\Delta_{pv}\nu = \nu^{(R)} - \nu^{(S)}$ for comparable spectroscopic transitions observed in the left and right handed enantiomers. Fig. 1 illustrates this approach in comparison with the measurement of $\Delta_{pv}E$ itself.

In this energy level scheme of Fig. 1 the overall ground rovibronic state corresponds to the (S) enantiomer, whereas the (R) enantiomer has its ground state at an energy higher by $\Delta_{pv}E$ (in the high barrier limit, see [16]). The measurement of $\Delta_{pv}E$ relies on transitions to an excited state of well defined parity ("+" in Fig. 1, or at least sufficient excess parity), which connects optically to both (R) and (S) ground state levels [16, 17]. As a rule, by this technique one will obtain the maximum parity violating effect, which at the same time is a fundamental thermodynamic quantity, the enthalpy of the reaction at 0 K

$$S \rightleftharpoons R \qquad \Delta_{pv}E = \Delta_r H_0^0/N_A \,. \tag{1}$$

While this is quite small (for the example CHBrClF of the present paper

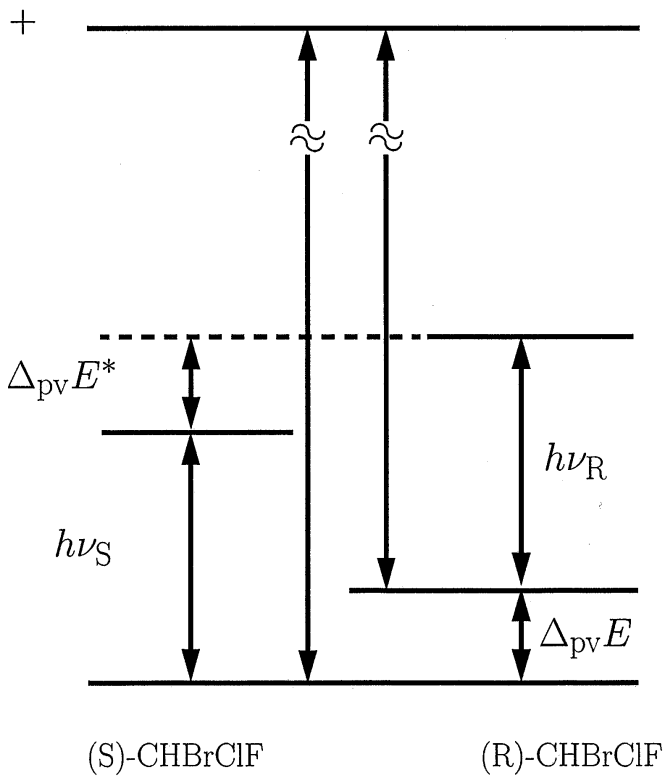

Fig. 1. Energy level scheme for a (R) enantiomer (right) and a (S) enantiomer (left) with an energy separation due to parity violation of $\Delta_{pv}E$ (vibrational ground state) and $\Delta_{pv}E^*$ (excited vibrational state) and the fundamental absorptions with transition energies of $h\nu_R$ and $h\nu_S$. We indicated transitions to an excited state with a definite parity, here positive. See text for discussion.

we calculate to be about 10^{-11} J mol^{-1}), the other effects based on the second approach to molecular parity violation to be discussed now, will be even smaller, in general. This approach measures a transition frequency in either the (S) enantiomer or the (R) enantiomer and compares the two. Because as a rule the excited levels will be separated by $\Delta_{pv}E^*$ very similar to $\Delta_{pv}E$ the measurable $h|\nu^{(R)} - \nu^{(S)}|$ will be smaller than $|\Delta_{pv}E|$, although exceptions to this rule are conceivable (the spectroscopic measurement of $\Delta_{pv}E$ via a common intermediate level discussed above is an obvious exception). As we shall see below, $h|\nu^{(R)} - \nu^{(S)}|$ can be on the order of 10% of $\Delta_{pv}E$ for vibrational transitions in the example CHBrClF. Measurements of $\nu^{(R)} - \nu^{(S)}$ have been proposed (and carried out) in a variety of spectral ranges from radiofrequency (NMR) [34], to microwave rotational spectra

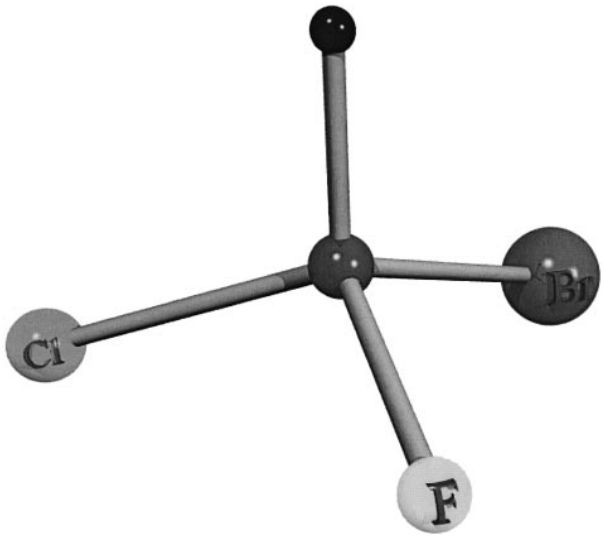

Fig. 2. Graphical representation of (R)-CHBrClF for the equilibrium structure. The *ab initio* calculated internal coordinates [35] in the ordering of r_e^0(CH), r_e^0(CF), r_e^0(CCl), r_e^0(CBr), φ_e^0(HCF), φ_e^0(HCCl), φ_e^0(HCBr), φ_e^0(FCCl), φ_e^0(ClCBr) are as follows (bond lengths in Å, bond angles in degrees): 1.0807, 1.3609, 1.7529, 1.9220, 108.43, 108,51, 108.29, 109.02, 113.38. The r_e^0 and φ_e^0 correspond to the equilibrium geometry on the zero order (parity conserving) potential hypersurface (see section 2.5).

[35], infrared vibrational spectra [35−43] and perhaps γ-ray (Mössbauer) spectra [44]. While early experiments generally were limited to a relative accuracy $\Delta\nu/\nu \approx 10^{-6}$ to 10^{-8} [35−40], a most recent experiment led to an accuracy $\Delta\nu/\nu \approx 4\times10^{-13}$ and thus a corresponding upper limit $\Delta\nu/\nu < 4\times10^{-13}$ in the ν_4 fundamental of CHBrClF [41, 42].

In view of these experiments, accurate calculations of parity violating shifts in rovibrational spectra of chiral molecules are of interest. An early paper has provided already some very approximate estimates [25]. It seems, however, that our recent effort is the first serious attempt at an accurate calculation of these effects in polyatomic molecules. Preliminary results from the present work have been reported at scientific meetings [45, 46]. Subsequent recent work based on a relativistic Dirac Fock approach (to be compared with RHF at the nonrelativistic level) seems to confirm that relativistic corrections are relatively modest even for molecules involving Br and Cl atoms [47].

This paper presents first a detailed account of the various theoretical approaches and problems related to the calculation of rovibrational frequency shifts due to parity violation in chiral molecules. We then present numerical results for the molecule CHBrClF (Fig. 2).

This molecule has been a prototype of chiral molecules for more than a century [48] and has been considered in the context of parity violation already in 1976 [39]. We have studied its rovibrational high resolution spectrum for almost a decade (see [35−38] and references cited therein) and have achieved the first rovibrational analysis of an infrared fundamental for any chiral molecule [35]. Based on our analysis of ν_4, spectra at ultrahigh resolution taken by Daussy *et al.* [41, 42] on this band led to the most stringent bound for $h|\nu^{(R)} - \nu^{(S)}|$ so far available.

2. Theory

2.1 Calculation of parity violating potentials in polyatomic molecules

A simple term in the molecular Hamiltonian that transforms odd under parity and thus leads to parity violating potentials is given by

$$\hat{H}_{pv} = -\frac{G_F}{2\sqrt{2}m_e c} \cdot \sum_{i,a} \left(N_a - Z_a\,(1-\sin^2(\theta_W))\right) \hat{\vec{s}}_i \cdot [\hat{\vec{p}}_i, \delta^3(\vec{r}_i - \vec{r}_a)]_+ \qquad (2)$$

where G_F is Fermi's coupling constant, m_e: electron mass, c: velocity of light, Z_a: nuclear charge of nucleus a, N_a: neutron number of nucleus a, θ_w: Weinberg angle $\sin^2(\theta_W) \approx 0.224(19)$ [49] (in the computations we still used the somewhat older value 0.2319 [27−30]), $\delta^3(\vec{r}_i - \vec{r}_a)$: Dirac's delta distribution, $\hat{\vec{s}}_i$: spin operator of electron i, $\hat{\vec{p}}_i$: momentum operator of electron i, and $[\ldots]_+$ denotes an anticommutator [20, 22, 28, 50]. The anticommutator is defined through its action on a wavefunction to its right by considering the chain rule. The three dimensional Dirac delta distribution is a product of three one dimensional Dirac delta distributions [51] and applied to Eq. (2) we obtain together with

$$\delta^3(\vec{r}_i - \vec{r}_a) = \delta(x_i - x_a)\delta(y_i - y_a)\,\delta(z_i - z_a) \qquad (3)$$

$$\int f(x_i) \frac{\partial^n}{\partial x_a^n} \delta(x_i - x_a)\,\mathrm{d}x_i = (-1)^n \frac{\partial^n}{\partial x_a^n} f(x_a) \qquad (4)$$

for a matrix element of the anticommutator (in x, e.g.)

$$\langle \Psi_a | [p_{x_i}, \delta(x_i - x_a)]_+ | \Psi_b \rangle = +\,i \left(\frac{\partial \Psi_a}{\partial x_i} \cdot \Psi_b|_{x_i = x_a} - \Psi_a \cdot \frac{\partial \Psi_b}{\partial x_i}|_{x_i = x_a} \right). \qquad (5)$$

Spin and spatial coordinates are completely separable. Eq. (5) shows that the parity violating contribution is related to the gradient of the wavefunction of the electron at the position of the nucleus (somewhat similar to the Fermi contact interaction in magnetic resonance [52], which is related to the square modulus of the wave function at the position of the nucleus).

An estimate of the parity violating potential V_{pv}, giving rise to energy difference between left- and right-handed enantiomers of a chiral molecule can be obtained from a sum-over-states expression (see [28], and refs. therein)

$$V_{pv} = 2 \cdot Re \sum_n \frac{\langle {}^1\Psi_0 | \hat{H}_{SO} | {}^3\Psi_n \rangle \cdot \langle {}^3\Psi_n | \hat{H}_{pv} | {}^1\Psi_0 \rangle}{{}^1E_0 - {}^3E_n} . \quad (6)$$

${}^1\Psi_0$ denotes the singlet electronic ground state wavefunction and ${}^3\Psi_n$ the n^{th} electronically excited triplet state wavefunction and ${}^1E_0$, ${}^3E_n$ the corresponding energies. The matrix elements of the spin-orbit operator $\hat{H}_{SO}$ (see e.g. [28, 30, 53]) and $\hat{H}_{pv}$ are evaluated at cartesian geometries derived from a set of suitable non-redundant internal or reduced dimensionless normal coordinates (see below). The matrix elements for the spin-orbit and the parity-violating part are evaluated in a Gaussian-type atomic orbital basis and transformed to the molecular orbital basis set with the transformation matrix evaluated *ab initio*, e.g. with Gaussian 94 [54] in the restricted Hartree-Fock (RHF) approximation or configuration interaction with singly excited determinants (CIS) along the lines described in [28]. Due to convergence problems of the sum-over-states expression, especially when CIS is used, we implemented a new approach to calculate V_{pv} in the framework of the multi-configurational linear-response (MC-LR) approximation [30] making use of DALTON [55, 56]. DALTON allows to select several high-quality wavefunctions for which the linear response equations can be solved; E_{pv} is obtained from the linear response of H_{pv} to the perturbation H_{SO} at zero frequency [30]. Besides RHF we use in the present work the random-phase approximation (RPA) and a MC-LR version of the complete active space self-consistent field (CASSCF) approach. More details and a description and discussion of approximations made to evaluate V_{pv} in our work can be found elsewhere [27−30].

2.2 General theory of rovibrational frequency shifts in polyatomic molecules due to parity violation

The influence of the parity violating potential on the vibrational and rotational frequencies can be determined once the potential V_{pv} is known in some suitable non-redundant set of $3N - 6$ coordinates, where N is the number of atoms in the molecule. Suitable sets of coordinates are internal coordinates such as bond-lengths and bond-angles or normal coordinates. The latter have the distinct advantage of constituting a rectilinear coordinate system which offers considerable simplifications for the formulation of the vibrational Hamiltonian. A detailed discussion of the different choice of coordinate systems can be found in [36−38, 57−59].

As described in detail in our earlier work on the evaluation of multi-dimensional anharmonic potential energy surfaces for molecules with an

isolated CH chromophore [57, 60, 61], dimensionless reduced normal coordinates q_j (j from 1 to $3\,N-6$) are a good choice for treating rovibrational levels of strongly bound molecules at not too high excitations. In the case of N-atomic molecules one set of values for all normal coordinates corresponds to a set of $3\,N$ cartesian coordinates for the atoms (implying a convention for the center of mass position and rotation). We obtain reduced normal coordinates q_j from the diagonalization of the cartesian mass-weighted force constant matrix $\boldsymbol{F}^{(x,m)}$

$$q_j = \gamma_j^{1/2} \cdot \sum_n l_{nj} \cdot m_n^{1/2} \cdot x_n \tag{7}$$

with $\gamma_j = \sqrt{\omega_j}/\hbar$ where l_{nj} are the eigenvectors and ω_j are related to the eigenvalues; m_n are the atomic masses and x_n the atomic cartesian coordinates. We determine $V_{\mathrm{pv}}(\bar{q})$ along the reduced normal coordinates from the cartesian displacements [58]

$$\Delta x_n^{(j)} = \gamma_j^{-1/2} \cdot l_{nj} \cdot m_n^{-1/2} \cdot \Delta q_j \tag{8}$$

which define new cartesian geometries for elongation along q_j. These are then used to calculate $V_{\mathrm{pv}}(\bar{q})$ as described in the previous section.

The complete vibrational Hamiltonian can be written as

$$\hat{H}(\hat{\bar{p}},\bar{q}) = \hat{T}(\hat{\bar{p}},\bar{q}) + V(\bar{q}) + \hat{H}_{\mathrm{pv}}(\bar{q}) = \hat{H}^0(\hat{\bar{p}},\bar{q}) + V_{\mathrm{pv}}(\bar{q}) \tag{9}$$

where $\hat{T}$ and V are the kinetic and potential energy operators, and V_{pv} denotes the very small perturbation to the zeroth order Hamiltonian $\hat{H}^0$ due to parity violation (see Eq. (2)). The coordinate vector $\bar{q}$ has components $\{q_i\}$, $i = 1 \cdots 3N-6$; the $\hat{\bar{p}}_i$ are the conjugate momenta. The solution of the zeroth order Schrödinger equation

$$\hat{H}^0|\phi_n\rangle = E_n^0|\phi_n\rangle \tag{10}$$

provides the n^{th} eigenvalue E_n^0 and the corresponding eigenfunction $|\phi_n\rangle$. If $|\Psi_n\rangle$ denotes the eigenfunction of $\hat{H}$,

$$\hat{H}|\Psi_n\rangle = E_n|\Psi_n\rangle \tag{11}$$

in general this needs now diagonalization of the full Hamiltonian. To a good approximation, the first order correction to the zeroth order energy, E_n^0, is given by

$$E_n^{(1)} \approx \langle\phi_n|V_{\mathrm{pv}}|\phi_n\rangle\,. \tag{12}$$

For a given enantiomer, the energy shift due to the parity violating interaction is given by

$$E_n - E_n^0 \approx \langle\phi_n|V_{\mathrm{pv}}|\phi_n\rangle\,. \tag{13}$$

Correspondingly, the energy difference between enantiomers R and S is

$$\Delta_{\mathrm{pv}}E = E_n^{(\mathrm{R})} - E_n^{0(\mathrm{R})} - (E_n^{(\mathrm{S})} - E_n^{0(\mathrm{S})}) \approx 2\,\langle\phi_n|V_{\mathrm{pv}}|\phi_n\rangle\,. \tag{14}$$

Since the magnitude of the parity violating perturbation is very small, diagonal perturbation theory is expected to provide good estimates for the fre-

quency shifts as long as they remain small with respect to the zeroth order level separations. In principle, the matrix elements in Eq. (13) is to be calculated with a fully anharmonically coupled multi-dimensional vibrational (or more generally rovibrational) wavefunction ϕ_n. In practice some further approximations are useful.

2.3 Separable harmonic and anharmonic approximation for adiabatic vibrational frequency shifts

The multi-dimensional integral in Eq. (13) needs in a first stage the solution of the multidimensional anharmonic rovibrational problem with the Hamiltonian $\hat{H}^0$. Even with separation of rotation and vibration this type of problem has been solved exactly only for molecular problems with a maximum of six to nine vibrational degrees of freedom (see for example [62, 63]). The formulation of a fully coupled $3N-6$ dimensional anharmonic potential energy hypersurface for a chiral molecule represents a substantial task (see for example the formulation of methane potentials in [64]) and so would the formulation of a fully coupled V_{pv} for $3N-6$ degrees of freedom in chiral molecules. It seems natural to start out with a separable normal mode approximation for $\hat{H}^0$, and thus

$$\hat{H}^0 = \sum_{j=1}^{3N-6} \hat{H}_j^0(p_j,q_j) \tag{15}$$

$$E_n^0 = \sum_{j=1}^{3N-6} E_{n,j}^0 \tag{16}$$

$$\phi_n = \prod_{j=1}^{3N-6} \varphi_{n,j}(q_j) \tag{17}$$

where the sums (or the product) extend over all normal modes. In the strictly harmonic approximation, the $\varphi_{n,j}$ are harmonic oscillator functions. More generally one may solve the one-dimensional anharmonic Schrödinger equation on a grid [65] for each normal coordinate and obtain separable one dimensional anharmonic zero order energies $E_{n,j}^0$ and wavefunctions $\varphi_{n,j}(q_j)$ in each vibrational mode. The first order parity violating energy shift for each vibrational mode is then given by

$$E_{n,j} - E_{n,j}^0 \approx \langle \varphi_{n,j} | V_{\mathrm{pv}}(q_j) | \varphi_{n,j} \rangle \,. \tag{18}$$

In a further step one may include the most important vibrational anharmonic couplings, which leads typically to coupled three or four dimensional problems, which are difficult but still manageable and can be solved exactly on 3D and 4D grids [36, 66, 67].

In the present paper we restrict our attention to the one dimensional approximations. The relative vibrational frequency shift for a vibrational transition in mode j between two enantiomers is then given by

$$\Delta_{\mathrm{pv}} v_j^{\mathrm{ul}} / v_j^{\mathrm{ul}} = 2\,(\langle v_j^{\mathrm{u}} | V_{\mathrm{pv}}(q_j)/hc | v_j^{\mathrm{u}} \rangle - \langle v_j^{\mathrm{l}} | V_{\mathrm{pv}}(q_j)/hc | v_j^{\mathrm{l}} \rangle)/\tilde{x}_j^{\mathrm{ul}} \tag{19}$$

where v_j^{u} denotes the perturbed upper vibrational level, v_j^{l} the corresponding lower vibrational level and $\tilde{x}_j^{\mathrm{ul}}$ is the wavenumber term difference between two levels in mode j. For vibrational fundamentals this is denoted $\tilde{\nu}_j$ (anharmonic) or $\tilde{\omega}_j$ (harmonic).

2.4 Reverse adiabatic harmonic approximation for vibrational frequency shifts

One may furthermore approximate the anharmonic vibrational fundamental frequency shift between enantiomers, $\Delta_{\mathrm{pv}} \nu_j$, by the shift of the harmonic frequencies arising from the apparent change of the effective force constants in the normal coordinate q_j due to the parity violating potential:

$$\tilde{\omega}_j \approx \tilde{\omega}_j^0 + \Delta_{\mathrm{pv}} \tilde{\omega}_j \tag{20}$$

$$\Delta_{\mathrm{pv}} \tilde{\nu}_j \approx \Delta_{\mathrm{pv}} \tilde{\omega}_j \, (\tilde{\nu}_j / \tilde{\omega}_j^0) \approx \frac{2}{hc} \cdot [l_0^{\dagger} F_{\mathrm{pv}} l_0]_{jj} \, (\tilde{\nu}_j / \tilde{\omega}_j^0) \tag{21}$$

where l_0 diagonalizes the cartesian force constant matrix $F^{(\alpha,m)}$ with eigenvalues related to $\tilde{\omega}_j^0$. The factor 2 has been introduced because we consider the difference between enantiomers (denoted with Δ_{pv}, see Eq. (14)). In this approach we find

$$\tilde{\omega}_{\mathrm{R}} - \tilde{\omega}_{\mathrm{S}} = \Delta_{\mathrm{pv}} \tilde{\omega}_j \approx 4 \cdot p_2(j) \tag{22}$$

where the coordinate dependent *ab initio* parity violating potential V_{pv} has been fitted by a least-squares procedure to a polynomial expansion up to n^{th} order

$$\frac{V_{\mathrm{pv}}(q_j)}{hc} = \sum_{k=0}^{n} p_k(j) \, q_j^k \,. \tag{23}$$

In practice a third order expansion in Eq. (23) turns out to be sufficient.

This treatment actually corresponds to a model that interprets the parity violating effect as arising from a *kinetic energy* as well as from a *potential energy* contribution arising by effectively a reverse adiabatic approximation [45].

2.5 Approximate theory of rotational frequency shifts and structural changes in polyatomic molecules due to parity violation

2.5.1 Structural changes

The vibrational potential energy V is modified by the parity violating potential V_{pv} and gives rise to a new global minimum which is shifted with

respect to the minimum of the parity conserving potential (in reduced normal coordinates, the latter corresponds to $V\,(q_1 = 0,\, q_2 = 0, \cdots,\, q_9 = 0)$, which in internal coordinates corresponds to $V(r_e^0(\mathrm{CH}),\, r_e^0(\mathrm{CF}),\, r_e^0(\mathrm{CCl}),\, r_e^0(\mathrm{CBr}),\, \varphi_e^0(\mathrm{HCF}),\, \varphi_e^0(\mathrm{HCCl}),\, \varphi_e^0(\mathrm{HCBr}),\, \varphi_e^0(\mathrm{FCCl}),\, \varphi_e^0(\mathrm{ClCBr}))$, determined without V_{pv} present. This change in equilibrium geometry induces a change of the rotational constants A_e, B_e, C_e which can be used to estimate the shifts on the pure rotational spectrum observable in the microwave region. Again, a general theory of the structure changes would require a minimum search on a $3N - 6$ dimensional potential energy hypersurface. This can be reduced by restriction to a more limited space, which can be chosen in several ways corresponding to different approximations. We discuss here in detail those results obtained with dimensionless reduced normal coordinates and refer more briefly to results in a non-redundant set of internal bond-lengths, bond-angles coordinates and other approximations when appropriate. For each vibrational mode (uncoupled, but due to V_{pv} no longer harmonic), we have a coordinate dependence (expressed in reduced normal coordinates of the molecular system without V_{pv} present) according to (see Eq. (23))

$$\frac{V(q)}{hc} = \frac{1}{2}\,\tilde{\omega}\,q^2 + \sum_{i=0}^{3} p_k\,q^k\,. \tag{24}$$

The coordinate for the new minimum is approximately given by the expression

$$q_{j\min} \approx -\frac{p_1(j)}{\tilde{\omega}_j^0 + 2\,p_2(j)} \approx -\frac{p_1(j)}{\tilde{\omega}_j^0} \tag{25}$$

which gives directly the shift with respect to $q_j = 0$ and corresponds to a change in cartesian geometry. From this change of the cartesian geometry caused by V_{pv} we can also estimate a change of the bond lengths and bond angles. From the definition of the distance r_{ij} between two atoms i and j

$$r_{ij}^2 = (x_i - x_j)^2 + (y_i - y_j)^2 + (z_i - z_j)^2 \tag{26}$$

we obtain

$$\Delta r_{ij} \approx \frac{(x_i^0 - x_j^0)(\Delta x_i - \Delta x_j) + (y_i^0 - y_j^0)(\Delta y_i - \Delta y_j) + (z_i^0 - z_j^0)(\Delta z_i - \Delta z_j)}{r_{ij}^0}$$

$$r_{ij} \approx r_{ij}^0 + \Delta r_{ij} \tag{27}$$

by again neglecting nonlinear terms in Δ. From the parity violating potential we thus have a linear perturbation Δr_{ij} to the equilibrium bond length r_{ij}^0 (without V_{pv} present) which can be estimated by this procedure. The bond angle φ between three atoms denoted 1-2-3 (with the central atom 2) is

given by

$$\cos(\varphi^0 + \Delta\varphi) \approx \frac{\sum_{\alpha=(x,y,z)} [(\alpha_1^0 - \alpha_2^0)(\alpha_3^0 - \alpha_2^0]}{r_{21}^0 r_{23}^0 (1 + \Delta r_{23}/r_{23}^0 + \Delta r_{21}/r_{21}^0)} + \frac{\sum_{\alpha=(x,y,z)} [(\alpha_1^0 - \alpha_2^0)\Delta\alpha_{23} + (\alpha_3^0 - \alpha_2^0)\Delta\alpha_{21}]}{r_{21}^0 r_{23}^0 (1 + \Delta r_{23}/r_{23}^0 + \Delta r_{21}/r_{21}^0)}. \tag{28}$$

We have to a reasonably good approximation for small $\Delta\varphi$ (for example, y would correspond to $\Delta\varphi$ which is on the order of 10^{-15})

$$\arccos(x+y) \approx \arccos(x) + \arccos(y) - \frac{\pi}{2} \tag{29}$$

$$\arccos(a \cdot y) \approx a \cdot \arccos(y) + \frac{\pi}{2} \tag{30}$$

and consequently, the change of the bond angle, $\Delta\varphi$, in its linear approximation is

$$\Delta\varphi \approx \arccos\left[\frac{\sum_{\alpha=(x,y,z)} [(\alpha_1^0 - \alpha_2^0)\Delta\alpha_{23} + (\alpha_3^0 - \alpha_2^0)\Delta\alpha_{21}]}{r_{21}^0 r_{23}^0}\right]. \tag{31}$$

The approximate expressions to determine Δr and $\Delta\varphi$ have been checked by calculating the exact change from cartesian coordinates using high precision arithmetic from MAPLE [68] with 70 digits. The results differ by less than 10 percent.

2.5.2 Changes in the moment-of-inertia tensor

The (symmetric) moment-of-inertia tensor in the center-of-mass system (CM) is given by [69]

$$I = \begin{pmatrix} I_x & -D_{xy} & -D_{xz} \\ -D_{xy} & I_y & -D_{yz} \\ -D_{xz} & -D_{yz} & I_z \end{pmatrix} \tag{32}$$

where the diagonal element I_x (and similarly I_y, I_z) is given by

$$\begin{aligned} I_x &= \sum_\alpha m_\alpha [(x_{\alpha,y} + \Delta x_{\alpha,y})^2 + (x_{\alpha,z} + \Delta x_{\alpha,z})^2] \\ &\approx \sum_\alpha m_\alpha [x_{\alpha,y}^2 + x_{\alpha,z}^2] + 2\sum_\alpha m_\alpha [x_{\alpha,y}\Delta x_{\alpha,y} + x_{\alpha,z}\Delta x_{\alpha,z}] \\ &\approx I_x^0 + 2\sum_\alpha m_\alpha [x_{\alpha,y}\Delta x_{\alpha,y} + x_{\alpha,z}\Delta x_{\alpha,z}] \\ &\approx I_x^0 + \Delta I_x \end{aligned} \tag{33}$$

and the off-diagonal element D_{xy} (similarly for D_{xz} D_{yz}) by

$$\begin{aligned} D_{xy} &= \sum_{\alpha} m_\alpha \, (x_{\alpha,x} + \Delta x_{\alpha,x}) \, (x_{\alpha,y} + \Delta x_{\alpha,y}) \\ &\approx D^0_{xy} + \sum_{\alpha} m_\alpha \, [x_{\alpha,x} \Delta x_{\alpha,y} + x_{\alpha,y} \Delta x_{\alpha,x}] \\ &\approx D^0_{xy} + \Delta D_{xy} . \end{aligned} \tag{34}$$

The summation is over the N atoms, $\alpha = 1 \cdots N$, and Δx denotes the change in cartesian coordinates due to V_{pv}. We neglected quadratic and higher terms in Δf ($f = D,I,x$) since $\Delta f/f$ itself is on the order of 10^{-15}. This form gives the change in the moment of inertia, $\Delta \mathbf{I}$ as a linear perturbation to $\mathbf{I}^0$ with a common scaling factor, and is therefore well suited for numerical evaluation again without any loss of precision. The cartesian change in geometry due to the shift in reduced normal coordinates is given by Eq. (8) in this approximation.

2.5.3 Changes in the rotational constants

The rotational constants A_{e}, B_{e}, C_{e} are inversely proportional to the eigenvalues of the inertial tensor, i.e.

$$\mathbf{Z}^{\mathrm{T}} \mathbf{I} \mathbf{Z} = \mathrm{diag}(I_A, I_B, I_C) \tag{35}$$

$$X_{\mathrm{e}} = \frac{h}{8 \, \pi^2 c I_X} \tag{36}$$

with $X = A,B,C$. Rigorously one has thus the zero order ("parity conserving") rotational constants from

$$\mathbf{Z}_0^{\mathrm{T}} \mathbf{I}_0 \mathbf{Z}_0 = \mathrm{diag}(I^0_A, I^0_B, I^0_C) \tag{37}$$

and the rotational constants including parity violation from

$$\mathbf{Z}^{\mathrm{T}} (\mathbf{I}_0 + \Delta \mathbf{I}) \mathbf{Z} = \mathrm{diag}(I^0_A + \Delta I_A, I^0_B + \Delta I_B, I^0_C + \Delta I_C) \, . \tag{38}$$

Because ΔI_A, ΔI_B, ΔI_C are very small, one can use the following approximation to calculate the changes in rotational constants: We assume that the diagonal elements I^{xx}_{pv} (where x labels the three diagonal elements as a,b,c) of $\mathbf{Z}_0^{\mathrm{T}} \Delta \mathbf{I} \mathbf{Z}_0$ provides an estimate for the change in the principal moments of inertia $\mathbf{I}^0_X$, where $\mathbf{Z}_0$ is the eigenvector matrix obtained by diagonalizing $\mathbf{I}^0$. If we denote the rotational constant obtained by diagonalizing $\mathbf{I}^0 + \Delta \mathbf{I}$ by X_{e} following Eqs. (35), (36) we have

$$\begin{aligned} X_{\mathrm{e}} &\approx X^0_{\mathrm{e}} + \Delta X_{\mathrm{e}} \\ &\approx X^0_{\mathrm{e}} \cdot (1 - I^{xx}_{\mathrm{pv}}/I^0_X) \, . \end{aligned} \tag{39}$$

Thus we have

$$\Delta X_{\mathrm{e}}/X^0_{\mathrm{e}} = (X_e/X^0_{\mathrm{e}}) - 1 \approx - X^0_{\mathrm{e}}/X_{\mathrm{pv}} = - I^{xx}_{\mathrm{pv}}/I^0_{\mathrm{X}} \tag{40}$$

where $X_{\mathrm{pv}} = h/(8 \, \pi^2 c I^{xx}_{\mathrm{pv}})$. Again, the approximate expressions have been

checked with MAPLE [68] and no deviations where found for the values presented here. The microwave spectral changes are related to the changes of rotational energy levels. While there are no simple expressions for asymmetric tops (where all rotational constants are different), the leading terms in the energy level expressions can be estimated from expressions of the kind

$$E_J \approx (hc)\, C_0\, J(J+1) + \cdots \tag{41}$$

with total angular momentum quantum number J, and a selection rule $\Delta J = \pm 1$ transition wavenumbers are of the order

$$\tilde{\nu} \approx 2\, C_0\, J + \cdots \tag{42}$$

and relative frequency shifts

$$\frac{\Delta\tilde{\nu}_{\mathrm{rot}}}{\tilde{\nu}_{\mathrm{rot}}} \approx \frac{\Delta C_0}{C_0}\,. \tag{43}$$

Here C_0 is the effective rotational constant in the vibrational ground state and ΔC_0 the corresponding shift due to parity violation. These are not easily calculated, as they again require the solution of a multidimensional rovibrational Schrödinger equation [62]. However, consistent with other approximations we may use

$$\frac{\Delta\tilde{\nu}_{\mathrm{rot}}}{\tilde{\nu}_{\mathrm{rot}}} \approx \frac{\Delta C_0}{C_0} \approx \frac{\Delta C_{\mathrm{e}}}{C_{\mathrm{e}}} \tag{44}$$

where ΔC_{e} and C_{e} are directly available from the above calculations. Exact solutions for rotational transitions (including even rovibrational couplings) would be possible in principle [70], but are hardly required at the present level of approximation. The changes $\Delta\mathbf{I}$ and $\Delta A(\Delta B, \Delta C)$ discussed in the present section 2.5 all refer to changes from the (R) enantiomer (which we used throughout the calculations, except when explicitely stated otherwise) when including the parity violating potential with respect to the parity conserving result. In order to obtain differences $\Delta_{\mathrm{pv}}X$ that exist between (R) and (S) enantiomers, $\Delta_{\mathrm{pv}} = \Delta^{(\mathrm{R})} - \Delta^{(\mathrm{S})}$, one may multiple ΔX by 2, for example

$$\Delta_{\mathrm{pv}} C_{\mathrm{e}} = \Delta C_{\mathrm{e}}^{(\mathrm{R})} - \Delta C_{\mathrm{e}}^{(\mathrm{S})} \approx 2\, \Delta C_{\mathrm{e}}^{(\mathrm{R})}\,. \tag{45}$$

This has also been verified numerically.

3. Results and discussion

CHBrClF is a chiral molecule which has already been investigated, both, spectroscopically and theoretically by high-resolution Fourier-Transform vibrational overtone spectroscopy in the infrared range for the isolated CH chromophore presented elsewhere [36−38, 71]. To determine the normal

Table 1. Harmonic vibrational wave numbers ω in cm^{-1} for CHBrClF; Basis 1: 6-311+G(d,p); Basis 2: 6-311+G(2d,2p); Basis 3: 6-311+G(2df,2pd); Basis 4: from refs. [36, 37, 71] obtained with a basis set of essentially double-zeta quality; Basis 5: VDZ [74]. Basis 4 has been used to determine the normal coordinates and Basis 5 has been used for V_{pv} calculations. The second column are anharmonic vibrational fundamental wavenumbers [37]. Total electronic energies E_{tot} are quoted as $E_{tot}/E_h = E_{MP2}/E_h + 3170$.

	ν^{exp} [37]	Basis 1	Basis 2	Basis 3	Basis 4 [36,37,71]	Basis 5
ν_1	3025.5	3197	3223	3195	3245	3211
ν_2	1306.2	1354	1341	1337	1375	1290
ν_3	1202.8	1278	1242	1243	1315	1229
ν_4	1077.2	1092	1085	1107	1098	1032
ν_5	787.0	833	796	820	838	708
ν_6	663.6	684	669	684	680	619
ν_7	425.2	438	428	436	437	373
ν_8	313.0	324	319	323	327	300
ν_9	223.6	237	229	231	240	217
E_{tot}/E_h		−0.903291	−0.983025	−1.096614	−0.124477	0.404182

coordinates, we used the vibrational force field $F^{(x,m)}$ obtained at the level of second order Møller-Plesset perturbation theory (MP2) with basis 1 from our previous investigations [37]. This basis set is of double-zeta quality. We evaluated the coordinate dependence of $V_{pv}(q_j)$ for wavefunctions from Hartree-Fock theory (RHF, [28]), the random-phase approximation (RPA, [30]) and complete-active space SCF (CASSCF, [30]), the latter only for some selected vibrational modes. Except for the RHF wavefunction, the other high quality wavefunctions have been used together with the multi-configuration linear-response approach (MC-LR) described in detail elsewhere [30]. The results for vibrational frequencies from parity conserving potentials are summarized in Table 1. The parameters of the least-squares fit to describe the coordinate dependence of the parity violating potentials are listed in Table 2 for the nine vibrational modes.

3.1 Harmonic vibrational effects induced by parity violation

Table 1 summarizes the calculated harmonic vibrational frequencies obtained from MP2 calculations using different basis sets. The normal coordinates obtained from basis 4 have been used to determine the potential energy surface of the CH chromophore [37]. They define the reduced normal coordinate space for the present study of the parity violating potential. We use basis 5 for the pure electronic part of the *ab initio* calculation of the parity violating potential.

The dependence of the parity violating potential $V_{pv}(q_j)$ of (R)-CHBrClF on reduced normal coordinates is presented in Fig. 3 for all vibrational de-

Table 2. Polynomial fit coefficients p_i and root-mean-square deviation d_{rms} (all in 10^{-15} cm^{-1}) for ν_1 to ν_9 obtained with RPA (random-phase approximation) for the (R)-CHBrClF enantiomer. In parenthesis, the numerical uncertainty due to the least-squares procedure is given in units of the last significant digits.

Mode	p_0	p_1	p_2	p_3	d_{rms}
1	958.679(47)	33.219(91)	−6.746(26)	−0.488(29)	0.118
2	958.062(446)	680.124(869)	114.879(251)	8.010(274)	1.120
3	958.441(463)	1175.441(903)	−98.752(261)	−2.099(284)	1.163
4	958.799(31)	−294.061(60)	16.791(17)	0.1333(189)	0.077
5	958.754(7)	331.877(14)	−62.857(4)	0.799(5)	0.019
6	958.772(13)	−180.438(25)	20.187(7)	−1.345(8)	0.033
7	958.720(21)	637.852(41)	7.890(12)	−0.447(13)	0.053
8	958.791(25)	839.356(48)	−4.811(14)	0.396(15)	0.062
9	958.707(30)	−166.116(59)	−2.315(17)	−0.125(18)	0.075

grees of freedom. We have plotted the one-dimensional functions of $V_{pv}(q_j)$ from RPA in the reduced normal coordinate range $-2 \leq q_j \leq +2$. This can be converted to a normal coordinate range for Q_j with $Q_j/[\text{Å}\sqrt{\text{u}}] \approx q_j \cdot \sqrt{33.71527/[\tilde{\omega}_j/\text{cm}^{-1}]}$.

The variation of V_{pv} with q_j is qualitatively similar for both, the RHF and the RPA calculations, however, there are quantitative differences which can be seen from the results listed in Table 3.

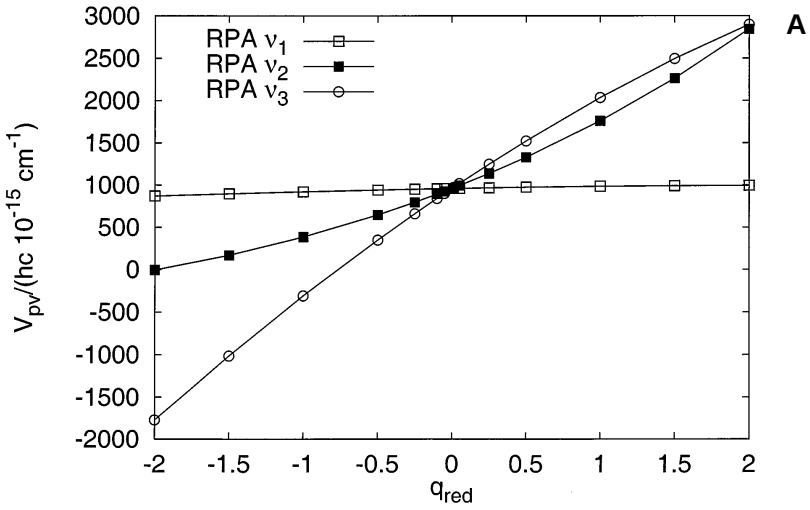

Fig. 3A

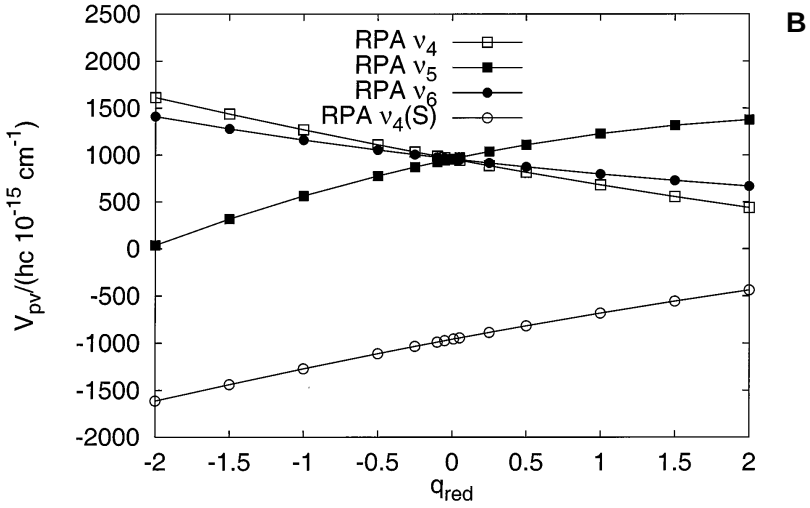

Fig. 3B

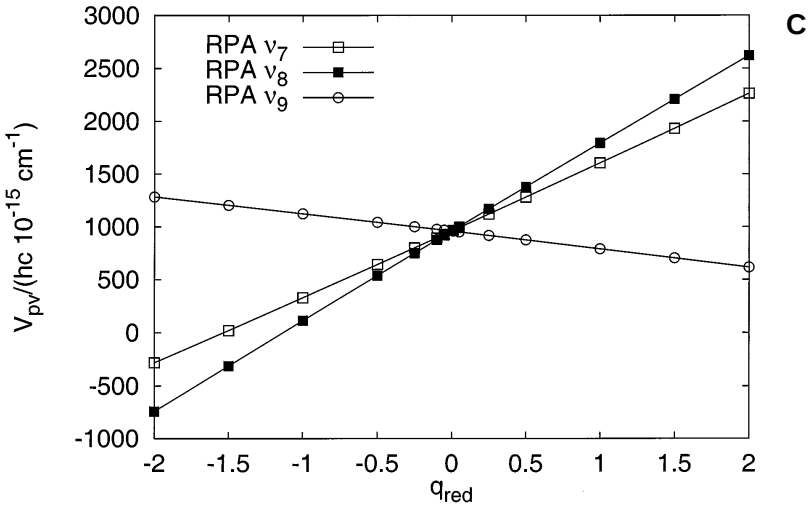

Fig. 3C

Fig. 3a–c. Dimensionless reduced normal coordinate dependence (q_{red}) of the parity violating potential $V_{pv}(q_{red})/hc$ in units of 10^{-15} cm^{-1} for three different vibrational modes: (a) ν_1 (open squares), ν_2 (filled squares), ν_3 (open circles), (b) ν_4 (open squares), ν_5 (filled squares), ν_6 (filled circles), $\nu_4^{(S)}$ (open circles), and (c) ν_7 (open squares), ν_8 (filled squares), ν_9 (open circles). All potentials have been calculated within the random-phase approximation (RPA) and for (R)-CHBrClF, except in (b) where we have also plotted the calculated parity violating potential of (S)-CHBrClF for $\nu_4^{(S)}$ (open circles) which shows the sign changes in V_{pv} for different enantiomers.

The parity violating potential energy is almost constant over the whole q-range for the highest vibrational mode ν_1, corresponding to the CH-stretching vibration. Except for q_4, q_6 and q_9, all functions decrease with increasing reduced normal coordinate (for the phase convention see [36–38]). The bending modes ν_2, ν_3 (CH bend), ν_7 (ClCF bend) and ν_8 (BrCF bend) reach comparably large V_{pv} values for strong elongation along q (see Fig. 3). We have additionally calculated V_{pv} for the (S)-CHBrClF enantiomer. The fit gives, within numerical accuracy, the same magnitude but different signs for V_{pv}, as expected. $\Delta_{pv}E/hc$ at the equilibrium position is just given by $2 \cdot p_0$ which in case of RPA is about 873.68×10^{-20} $E_h \approx 1917.5 \times 10^{-15}$ hc cm^{-1}. The fits give the same values of p_0 for all modes within the uncertainties of the fits (see Table 2).

Fig. 4 shows a plot of the scaled parity violating potential (multiplied by a factor of 3×10^{-4}, see Fig. 3a and 3b) for the CF stretching mode ν_4 (Fig. 4a) and the FCBr bending mode ν_8 (Fig. 4b). A first set of data is represented by the filled squares, the line represents the polynomial fit function (differences are invisible at this scale) to these data. We then calculated a second set of data in the range corresponding to an extrapolation. The empty circles represent these separate results which lie well on the cautiously extrapolated fit, the quality of which is thus confirmed to be excellent. We show also the vibrational anharmonic wavefunction for the vibrational ground state (dotted line) and the first excited state (solid line). These wavefunctions from the anharmonic adiabatic diagonal approximation are to scale and normalized to one. An analysis of the normal coordinates of CHBrClF according to the potential energy distribution [72] $P(i,j) = F(i,i) \cdot l^2(i,j)/\sum_i [F(i,i) \cdot l^2(i,j)]$ shows, that the lowest vibrational mode is a heavy mixture of the internal coordinates for C–Br stretch and the angles between H–C–Br, F–C–Cl, and F–C–Br. However, many of the other modes have a relatively local character, such as ν_1 for CH stretching, ν_2, ν_3 for CH bending and ν_4 for CF stretching (see also [37]). Table 2 collects the polynomial fit parameters for the one dimensional parity violating potentials obtained with RPA and basis 5.

The second derivatives of the force constant matrix needed to determine $\Delta_{pv}\omega$ according to Eqs. (20) and (21) have been obtained by a fit of $V_{pv}(q)$ data obtained in the reduced normal coordinate range from -2 to $+2$ to a third order analytical polynomial expression with a least squares procedure. The quadratic term p_2 is a measure for the perturbation of the force constant by the parity violating potential. The root-mean-square value of the fit to 13 data points is slightly better than 10^{-16} cm^{-1}. The values obtained for the two CH bending modes (ν_2 and ν_3) have the largest uncertainties. All other parameters are statistically very well determined.

Within the reverse adiabatic, harmonic approximation, the largest relative shift in the harmonic vibrational frequencies due to the parity violating potential, as presented in Table 3, is obtained for the CH-bending and the

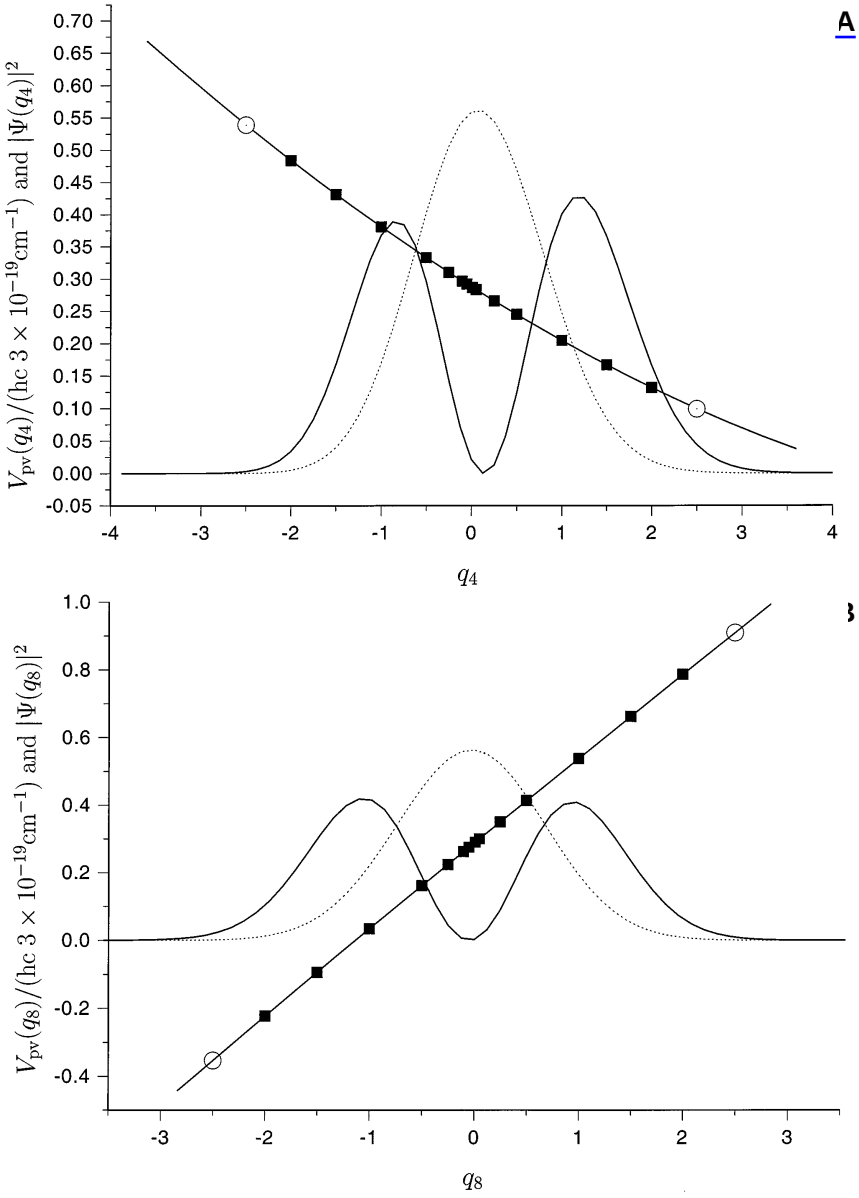

Fig. 4. Calculated $V_{pv}(q_{red})$ (points) from Fig. 3 (additionally multiplied by 3×10^{-4} for graphical representation) and the vibrational anharmonic one dimensional wavefunction for the vibrational ground state (dotted line) and first excited state (solid line) of (a) ν_4 and (b) ν_8. The filled squares correspond to the first set of *ab initio* data, the line is fitted by a least-squares procedure to a third order polynomial (see text), and the potential values at -2.5 and $+2.5$ (open circles) which lie outside the fitted range from -2.0 to $+2.0$ have been obtained from a separate *ab initio* calculation and thus confirm the extrapolated prediction from the fit.

Table 3. Harmonic vibrational wavenumbers $\tilde{\omega}$ (in cm^{-1}) and relative frequency shifts $\Delta_{pv}\tilde{\omega}/\tilde{\omega}$ in the reserve harmonic approximation (see Eq. (22)). The second column are anharmonic vibrational fundamental wavenumbers [71]. The third column provides harmonic frequencies from refs. [36, 37, 71] obtained with a basis set of essentially double-zeta quality.

j	$\tilde{\nu}_j^{exp}/cm^{-1}$ [37, 71]	ω_j/cm^{-1}	$\frac{\Delta_{pv}\omega_j}{\omega_j}\Big/10^{-19}$	
			RHF	RPA
1	3026	3245.000	−13.9	−83.2
2	1306	1375.227	+1134.0	+3341.4
3	1203	1315.363	−1173.3	−3003.1
4	1077	1097.851	+348.9	+611.8
5	787	838.309	−1613.6	−2999.2
6	664	680.406	+385.4	+1186.8
7	425	437.436	−498.5	+721.4
8	313	327.435	+490.9	−587.7
9	224	240.356	−150.5	−385.2

CCl-stretching vibrations. This applies to both calculations presented here, namely the sum-over-states expression in the RHF approach, as well as to the linear-response approximation in the RPA approach. Because the effect is so small (note the scaling of 10^{-19} for the relative shift, as given in Table 3), a direct experimental observation of the shift $\Delta\omega/\omega$ on the order of 10^{-16} is difficult (and so far unsuccessful [35−43]).

This, however, does not render the attempt to look for experimental evidence of the parity violating potential in vibrational spectra of molecules *a priori* hopeless. It has been discussed before that some excitation schemes to "achiral" levels of well defined parity might be a better approach to the signatures of parity violating effects in molecular systems [16, 17, 38, 73] (see also Fig. 1).

3.2 Role of the *ab initio* calculation

Table 4 shows the parameters from the fit of V_{pv} for the CF-stretching mode (ν_4) to the third order polynomial Eq. (23) for RPA and three high quality MC-LR(CASSCF) wavefunctions by steadily increasing the active space from 8 electrons distributed in 10 orbitals (denoted [8, 10]) to finally 12 electrons in 12 orbitals ([12, 12]), which is already a fairly large active space. The energy difference between the (R)- and the (S)-CHBrClF, $\Delta_{pv}E/hc$, is related to $2 \cdot p_0$, and the corresponding harmonic frequency shift $\Delta_{pv}\tilde{\omega}$ to $4 \cdot p_2$ in the reverse adiabatic harmonic approximation. The RPA seems to be a relatively good approximation. We also compare to the RHF-SDE

Table 4. Polynomial fit coefficients p_i and root-mean-square deviation d_{rms} (all in 10^{-15} cm^{-1}) for ν_4 obtained with different *ab initio* methods, namely RPA (random-phase approximation) and MC-LR CASSCF (multi-configuration linear response complete-active space SCF) for the (R)-CHBrClF enantiomer. In parenthesis, the numerical uncertainty due to the least-squares procedure is given in units of the last significant digits.

Method	p_0	p_1	p_2	p_3	d_{rms}
RHF	38.872(5)	−135.762(9)	9.575(2)	−0.1171(29)	0.012
RPA	958.799(31)	−294.061(60)	16.791(17)	0.1333(189)	0.077
[8,10] CAS	799.209(28)	−258.520(58)	18.656(17)	−0.1128(184)	0.076
[8,12] CAS	783.629(76)	−265.083(149)	19.474(43)	0.0704(468)	0.192
[12,12] CAS	962.698(45)	−246.650(87)	14.706(25)	0.0822(275)	0.113

approach in the first line of Table 4, which shows that the deficiency of RHF-SDE is substantial for p_0 (i.e. $\Delta_{pv}E$), as shown by us before for other molecules [27−30]. The effect on the higher coefficients p_1 to p_3, which determine the vibrational shift, is smaller.

3.3 Anharmonic effects

The harmonic model of calculating the frequency shift caused by the parity violating energy difference is approximate. A severe approximation is to neglect anharmonic contributions. From our investigation of the isolated CH-chromophore we know that diagonal and off-diagonal anharmonicity has a pronounced influence on the vibrational band positions and wavefunctions. A three-dimensional vibrational analysis based on *ab initio* potential energy surfaces revealed a strong anharmonic Fermi-resonance coupling between the CH-stretching motion and the two CH-bending motions. The relatively poor fit of V_{pv} for those modes (1−3, see Table 2) might be an indication that this coupling is also of some influence on V_{pv}. We discuss here first the diagonal anharmonic contribution to the parity violation induced frequency shift. This is achieved with 1st order perturbation theory by calculating the expectation value $\langle v'|V_{pv}|v'\rangle$ using *anharmonic* vibrational wavefunctions as discussed in section 2. The results are collected in Table 5.

The harmonic values in Table 5 have been obtained by calculating the expectation value with a harmonic vibrational potential energy. These harmonic shifts are a factor of 2 smaller than those reported in Table 3, as can be easily understood. Calculating the parity violation induced frequency shift from the force constants (see above) implies that the parity violation Hamiltonian is interpreted as a Hamiltonian with a kinetic and a potential energy. In case of a harmonic oscillator, the virial theorem connects the expectation value of the kinetic energy $\langle T\rangle$ with the expectation value of the

Table 5. Relative vibrational frequency shifts from expectation values (in 10^{-19}) according to Eq. (19) between (R)- and (S)-CHBrClF enantiomers. The parity violating potential is from RPA calculations (Table 2). (a) tabulated as $2(\langle 1|\tilde{V}_{pv}|1\rangle - \langle 0|\tilde{V}_{pv}|0\rangle)/\tilde{\omega}_1$ based on harmonic vibrational wavefunctions for the ground and first vibrationally excited state, $|0\rangle$ and $|1\rangle$; (b) tabulated as $2(\langle 1'|\hat{V}_{pv}|1'\rangle - \langle 0'|\hat{V}_{pv}|0'\rangle)/\tilde{\nu}_1$ based on anharmonic vibrational wavefunctions for the ground and first vibrationally excited state, $|0'\rangle$ and $|1'\rangle$.

Mode j	$\Delta_{pv}\nu_j^{1\leftarrow 0}/\nu_j^{1\leftarrow 0}$		Note
	harmonic[(a)]	anharmonic[(b)]	
1	−41.6	8.4	this work
2	1670.7	1319.2	this work
3	−1501.5	−1287.7	this work
4	305.9	−805.9	this work
	500.4	−623.0	[47]
5	−1499.6	−2499.5	this work
	−1853.1	−3028.5	[47]
6	593.4	952.9	this work
	186.3	522.0	[47]
7	360.7	1809.5	this work
8	−293.8	−3360.7	this work
9	−192.6	450.1	this work

potential energy $\langle V\rangle$ according to

$$\langle T\rangle = \langle V\rangle \tag{46}$$

and this explains the factor of two difference between the calculation of the frequency shift in the reverse adiabatic harmonic approximation and the adiabatic harmonic approximation as expectation value of the potential energy. Some of the shifts have recently also been calculated in the relativistic Dirac Fock framework [47]. As can be seen from Tables 5 and 3, the relativistic corrections are modest even for CHBrClF, containing Br as rather heavy atom. The harmonic Dirac Fock results in Table 5 should be compared to the harmonic RHF results in Table 3 (divided by 2). The corrections are modest, and no larger than the changes which result from going beyond the Hartree Fock level and from including anharmonicity.

We furthermore observe a strong dependence of the shift on anharmonic contributions. Table 6a and 6b offer detailed insight into the cause for the remarkable changes. Table 6a summarizes the expectation values for the ground state $\langle 0|\cdots|0\rangle$ and the first excited state $\langle 1|\cdots|1\rangle$ of the CF-stretching mode ν_4, and similarly Table 6b for ν_8. The second column in Table 6 are the polynomial parameters p_i (in 10^{-15} cm^{-1}, see Table 2). The expectation values for each individial polynomial term $p_i \cdot q^i$ (i = 0, 1, 2, 3) are listed separately. For harmonic oscillator wavefunctions the expectation value for odd powers of q is exactly zero and the quadratic term

Table 6a. Term-by-term analysis of expectation values contributing to the frequency shift in ν_4 as listed in Table 5 (see Eq. (19)) with anharmonic and harmonic vibrational wavefunctions for the vibrational ground and the first excited state (see also caption to Table 5).

i	p_i	$\langle 0\|p_i \cdot q^i\|0\rangle$	$\langle 1\|p_i \cdot q^i\|1\rangle$
Anharmonic wavefunctions			
0	958.80	958.80	958.80
1	−294.06	−31.02	−93.29
2	16.79	8.68	27.27
3	0.13	0.03	0.17
Sum		936.49	892.95
Harmonic wavefunctions			
0	958.80	958.80	958.80
1	−294.06	0.00	0.00
2	16.79	8.40	25.19
3	0.13	0.00	0.00
Sum		967.19	983.99

Table 6b. Term-by-term analysis of expectation values contribution to the frequency shift in ν_8 as listed in Table 5 (see Eq. (19)) with anharmonic and harmonic vibrational wavefunctions for the ground and the first excited state (see also caption to Table 5). This bending vibration shows the largest absolute shift, taking anharmonic contributions into account.

i	p_i	$\langle 0\|p_i \cdot q^i\|0\rangle$	$\langle 1\|p_i \cdot q^i\|1\rangle$
Anharmonic wavefunctions			
0	958.79	958.79	958.79
1	839.36	−30.35	−80.33
2	−4.81	−2.41	−7.27
3	0.40	−0.03	−0.15
Sum		926.00	871.05
Harmonic wavefunctions			
0	958.79	958.79	958.79
1	839.36	0.00	0.00
2	−4.81	−2.41	−7.21
3	0.40	0.00	0.00
Sum		956.40	951.48

increases with vibrational excitation. The contributions responsible for the strong difference between expectation values calculated from harmonic and anharmonic wavefunctions are the odd terms, particularly p_1. The absolute value of the anharmonic matrix elements of p_1 and p_3 increases with vibrational excitation.

Table 7. Anharmonic relative vibrational frequency shifts $\Delta\nu/\nu$ from expectation values (in 10^{-19}) according to Eq. (19) between (R)- and (S)-CHBrClF enantiomers for overtone transitions between the vibrational ground state (denoted 0) and the second, third and fourth vibrationally excited state for some modes ν_2 (CH bending), ν_4 (CF stretching), ν_5 (CCl stretching) and ν_6 (CBr stretching). The parity violating potential is from RPA calculations (Table 2).

Mode	ν_2	ν_4	ν_5	ν_6
Transition		$(\Delta_{pv}\nu/\nu)/10^{-16}$		
$2 \leftarrow 0$	+1.3389	−0.7806	−2.5382	+0.5934
$3 \leftarrow 0$	+1.3527	−0.7587	−2.5799	+0.5934
$4 \leftarrow 0$	+1.3547	−0.7492	−2.6177	+0.5934

3.4 Effects on overtone transitions

In Table 7 we summarize some vibrational frequency shifts for overtones of ν_2 (CH bending), ν_4 (CF stretching), ν_5 (CCl stretching) and ν_6 (CBr stretching).

Some modes show an increase of the relative anharmonic frequency shift (see Eq. (19)) upon overtone excitation (e.g., ν_2) whereas for ν_6 (CBr stretching) overtone excitation does not influence the relative shift at all. So far there is no obvious trend which would make a prediction possible without explicitely calculating the expectation values. It should be clear as well, that at higher vibrational excitations the one dimensional separable anharmonic approximation is unreliable and thus the present results are at best rough estimates.

3.5 Equilibrium structural effects and rotational frequency shifts

In Table 8 we collected the change in bond lengths and bond angles caused by parity violation. There is no obvious relation between the deviation of a bond length from its equilibrium value and the vibrational frequency shift. The approximate relation connecting the cartesian coordinate change with a change in bond angle, as derived above (column I, Table 8), is in good agreement with the exact value obtained by using MAPLE V [68] with high-precision arithmetic (column II). Following a different, more approximate route than presented here, the effect of parity violation on the molecular structure has been discussed in an early paper [25]. The parity violating effect on vibrational frequencies has therein been based on a discussion using *internal* bond-angle and bond-lengths coordinates thereby assuming that bond length and angles are parity-even whereas torsional and dihedral angles are parity-odd. It is clear, however, that this classification is erroneous in that parity transformation properties are connected only to *car-*

Table 8. Change in internal coordinates due to $V_{pv}(\vec{q})$ for the (R)-CHBrClF enantiomer determined in dimensionsless reduced normal coordinates. (I) Obtained with MAPLE V [68]; (II) obtained from the approximate expressions (see text for discussion); (III) obtained from (diagonal) $V_{pv}(\vec{r})$ determined in internal coordinates (see text for discussion). The definitions are $\Delta r_e = r_e(V + V_{pv}) - r_e(V)$ and $\Delta\varphi_e = \varphi_e(V + V_{pv}) - \varphi_e(V)$.

	Equilibrium [36, 37, 71]	Perturbed			
		RPA			RHF
		I	II	III	
	r/Å		$\Delta r/(10^{-19}$ Å)		
r(CH)	1.080 65	0.70	0.70	−4.84	5.0
r(CF)	1.360 85	198	198	181	68
r(CCl)	1.752 85	−397	−397	−366	−205
r(CBr)	1.922 02	62	62	178	44
	φ/degrees		$\Delta\varphi/(10^{-15}$ degrees)		
φ(HCF)	108.431	−5.70	−5.15	−2.1	−1.48
φ(HCBr)	108.289	−4.99	−4.69	−4.2	−2.70
φ(HCCl)	108.507	12.76	11.77	11.2	5.84
φ(FCCl)	109.024	−8.21	−7.94	−4.6	−5.03
φ(ClCBr)	113.382	−2.23	−2.50	−1.7	−0.06

tesian coordinates. An estimate for the equilibrium deviation in bond length on the order of 10^{-20} Å was presented [25], which is one to three orders of magnitude smaller than the results shown in Table 8. Our approach, however, is more consistent and extends the "independent mode approximation" briefly discussed in [25]. Column III in Table 8 summarizes those internal coordinates changes that are obtained by calculating the parity violating potential in a non-redundant set of internal coordinates. This set of internal coordinates consists of the following bond lengths and bond angles: r(CH), r(CF), r(CCl), r(CBr), φ(HCF), φ(HCCl), φ(HCBr), φ(FCCl), φ(ClCBr). They differ by two angles from those used in [37] to determine the harmonic force field. This choice has been made to facilitate an additional test of our results (see below). From the cartesian mass-weighted force constant matrix $\mathbf{F}^{(x,m)}$ we obtain the internal coordinates force constant matrix $\mathbf{F}^{\mathbf{int}}$ with the use of the contravariant tensor (Wilson's B-matrix) [58]

$$B_{k,i} = \frac{\partial S_k}{\partial x_i} \tag{47}$$

that transforms between cartesian (x_i) and internal (S_k) coordinates in matrix notation as

$$\mathbf{F}^{\mathbf{int}} = \mathbf{A}^{\top}\,\mathbf{F}^{(x,m)}\mathbf{A}$$
$$\mathbf{A} = \mathbf{M}^{-1}\mathbf{B}^{\top}(\mathbf{B}\,\mathbf{M}^{-1}\,\mathbf{B}^{\top})^{-1}\,. \tag{48}$$

Table 9. Rotational constants A_0, B_0, C_0 from experiment [35], A_e, B_e, C_e calculated *ab initio* [37] and calculated relative change of rotational constants $\Delta_{pv}X_e/X_e^0 = 2\,\Delta X_e/X_e^0 \approx -2\,X_e^0/X_{pv}$ (see Eqs. (40) and (45)) with $X = A, B, C$ due to parity-violating effects for RPA. There are no differences between the values in the last column and those obtained by diagonalizing the complete moment-of-inertia tensor using high precision arithmetic (MAPLE V, [68]), see text. Note that $\Delta X_e^{(R)} = -\Delta X_e^{(S)}$, which has been verified numerically (see text).

	Exp. [35]	*ab initio* (this work)	$\Delta_{pv}X_e/(X_e^0 \cdot 10^{-18})$
A/cm^{-1}	0.215 711 541 (23)	0.218 02	32.84
B/cm^{-1}	0.067 998 430 (14)	0.067 04	11.31
C/cm^{-1}	0.053 396 944 (16)	0.052 92	20.34

M denotes a $3\,N \times 3\,N$ diagonal matrix with the atomic masses. B is not a square matrix and can thus not be inverted. The cartesian force constant matrix is taken from *ab initio* calculations [37]. We have also carried out calculation with a nonseparable, explicitly coupled parity violating potential in the subspace of the three internal coordinates r(Cl), r(CBr), φ(CClBr). The results are similar to those in column III (Table 8), however with sizeable changes in a few instances.

Table 9 summarizes the relative change of the A,B,C rotational constants between both enantiomers caused by V_{pv}. This change is on the order of 10^{-17}. The separation of corresponding rotational transitions in both enantiomers is proportional to $\Delta_{pv}X = 2\Delta X$ and the rotational quantum number J. It should be made clear that because of the various approximations, the result for $\Delta_{pv}X$ in Table 9 must be considered order of magnitude estimates, not accurate predictions of rational line shifts, which would require inclusion of the anharmonic vibrational wave function [62].

4. Conclusions

From the present investigation we can draw the following main conclusions:

(i) The complete theory of parity violating rovibrational frequency differences between enantiomers of chiral molecules requires the solution of complicated multidimensional anharmonically and rovibrationally coupled problems. However, a first approximation is possible by reducing the problem to a set of one dimensional integrals over the parity violating potentials in terms of the molecular dimensionless reduced normal coordinate q_i.

(ii) The parity violating potentials can be expanded to an excellent approximation as a low order Taylor expansion.

(iii) The first term p_0 ($= \Delta_{pv} E/2$) is equal to half the parity violating energy difference between enantiomers and is much larger when calculated with MC-LR (CASSCF and RPA) approaches as compared to the traditional SDE-RHF approaches (more than a factor of 20 smaller for CHBrClF). This confirms our similar findings on the deficiency of SDE-RHF (on other molecules) which used both CIS and MC-LR approaches to prove this effect [27−30]. For CHBrClF the (S) enantiomer is calculated to be more stable than (R) by about 10^{-11} J mol^{-1}.

(iv) The higher terms of the Taylor expansion of $V_{pv}(q_i)$ govern the vibrational frequency shifts. They depend somewhat less strongly on the level of calculation (RHF versus MC-LR CASSCF and RPA). However, they do depend very strongly on the vibrational mode considered. The relative frequency shifts $\Delta_{pv}\nu/\nu$ fall in the range of $10^{-(16\pm1)}$ for CHBrClF.

(v) One finds a substantial difference between harmonic (both adiabatic and reverse adiabatic) and one dimensional anharmonic approximations for calculating the vibrational frequency shifts.

(vi) The exact calculation of structural changes leads again to very complicated multidimensional problems, which can be reduced to lower dimensionality only approximately. Different routes in this approximation lead to somewhat different predictions of structural changes, which are however of similar order of magnitude. Differences between RHF and RPA results are sizeable.

(vii) Using the structural changes with parity violation to predict differences between rotational frequencies of (R) and (S) enantiomers one finds values $\Delta\nu/\nu$ between 10^{-17} and 10^{-16}.

The present results show that all current experiments are still orders of magnitude away from the accuracy needed to achieve an observation of parity violating frequency shifts between (R)- and (S)-CHBrClF, say for the well analysed ν_4 band [35, 41, 42]. On the other hand, the strong vibrational mode dependence demonstrated here, together with the expected increase of the effects with heavy atom substitution, indicate that experimental observation of parity violating effects in rovibrational transitions may soon be possible. For such experiments, the careful prediction of the most suitable vibrational mode in a suitable molecule using the theoretical methods developed here should be helpful. However, even observation of these rovibrational frequency shifts will not provide the most important quantity, $\Delta_{pv}E$, as discussed in connection with Fig. 1. For this purpose, the kind of experiment proposed in [16, 17] with intermediate levels of preferred parity is necessary. For these more difficult experiments, the present calculations show a very large increase in predicted $\Delta_{pv}E$ compared to earlier expectations, which should render the effect more easily observable. Current work

is in progress in our laboratory towards experiments on suitable molecules as well as towards extending theory to treat more accurately the multidimensional rovibrational problems.

Acknowledgements

Substantial help from and discussions with Robert Berger are gratefully acknowledged as well as early advice (in spring 1998) by Peter Taylor on the DALTON program and discussions with Wim Klopper on relativistic effects (in summer 1999) and a recent preprint of [47] on these qustions by Peter Schwerdtfeger.

Our work is supported financially by ETH Zürich (including computer support through C4, Cray and CSCS) and the Schweizerischer Nationalfonds.

References

1. T. D. Lee and C. N. Yang, Phys. Rev. **104** (1956) 254.
2. C. S. Wu, R. W. Hayward, D. D. Hoppes and R. P. Hudson, Phys. Rev. **105** (1957) 1413.
3. S. Glashow, Nucl. Phys. **22** (1961) 579.
4. S. Weinberg, Phys. Rev. Lett. **19** (1967) 1264.
5. A. Salam, in Proceedings of the Eighth Nobel Symposium (edited by N. Svartholm), Amkvist and Wiksell, Stockholm (1968) 367.
6. R. E. Novick, *Thirty years of parity nonconservation*, Birkhäuser, Basel (1988).
7. M. Veltman. In: The Rise of the Standard Model, L. Hoddeson et al. (eds.) Cambridge U.P., Cambridge (1977) 145.
8. M.-A. Bouchiat and C. Bouchiat, Rep. Prog. Phys. **60** (1997) 1351.
9. I. B. Khriplovich, *Parity Nonconservation in Atomic Phenomena.* Gordon and Breach, Philadelphia (1991).
10. Y. Yamagata, J. Theoret. Biol. **11** (1966) 495.
11. D. Rein, J. Mol. Evol. **4** (1974) 15.
12. V. Letokhov, Phys. Lett. **A 53** (1975) 275.
13. B. Zel'dovich, Sov. Phys. JETP **9** (1959) 682.
14. B. Zel'dovich, D. Saakyan and I. Sobel'man, JETP Lett. **25** (1977) 94.
15. R. Harris and L. Stodolski, J. Chem. Phys. **73** (1980) 3862.
16. M. Quack, Angew. Chem. Int. Ed. Engl. **28** (1989) 571.
17. M. Quack, Chem. Phys. Lett. **132** (1986) 147.
18. M. Quack, Nova Acta Leopoldina, NF **81** (1999) 137.
19. D. W. Rein, R. A. Hegstrom and P. G. H. Sandars, Phys. Lett. **A71** (1979) 499.
20. R. A. Hegstrom, D. W. Rein and P. G. H. Sandars, J. Chem. Phys. **73** (1980) 2329.
21. S. F. Mason and G. E. Tranter, Chem. Phys. Lett. **94** (1983) 34.
22. S. F. Mason and G. E. Tranter, Mol. Phys. **53** (1984) 1091.
23. G. E. Tranter, Chem. Phys. Lett. **115** (1985) 286.
24. G. E. Tranter, Chem. Phys. Lett. **120** (1985) 93.
25. G. E. Tranter, Chem. Phys. Lett. **121** (1985) 339.
26. A. McDermott and G. Tranter, Chem. Phys. Lett. **163** (1989) 1.
27. A. Bakasov, T. K. Ha and M. Quack. In J. Chela-Flores and F. Rolin, editors, *Proc. of the 4th Trieste Conference (1995), Chemical Evolution: Physics of the Origin and Evolution of Life*, pages 287−296, Kluwer Academic Publishers, Dordrecht (1996).

28. A. Bakasov, T. K. Ha and M. Quack, J. Chem. Phys. **109** (1998) 7263; ibid. **110** (1999) 6081.
29. A. Bakasov and M. Quack, Chem. Phys. Lett. **303** (1999) 547.
30. R. Berger and M. Quack, J. Chem. Phys. **112** (2000) 3148.
31. P. Lazzeretti and R. Zanasi, Chem. Phys. Lett. **279** (1997) 349.
32. R. Zanasi and P. Lazzeretti, Chem. Phys. Lett. **286** (1998) 240.
33. J. Laerdahl and P. Schwerdtfeger, Phys. Rev. **A 60** (1999) 4439.
34. A. Barra, J. Robert and L. Wiesenfeld, Phys. Lett. A **115** (1986) 443.
35. A. Bauder, A. Beil, D. Luckhaus, F. Müller and M. Quack, J. Chem. Phys. **106** (1997) 7558.
36. A. Beil, D. Luckhaus, R. Marquardt and M. Quack, J. Chem. Soc. Faraday Discuss. **99** (1994) 49.
37. A. Beil, D. Luckhaus and M. Quack, Ber. Bunsenges. Phys. Chem. **100** (1996) 1853.
38. A. Beil, D. Luckhaus, M. Quack and J. Stohner, Ber. Bunsenges. Phys. Chem. **101** (1997) 311.
39. O. Kompanets, A. Kukudzhanov, V. Letokhov and L. Gervits, Opt. Commun. **19** (1976) 414.
40. E. Arimondo, P. Glorieux and T. Oka, Opt. Commun. **23** (1977) 369.
41. C. Daussy, Thèse de doctorat, Paris (1999).
42. C. Daussy, T. Marrel, A. Amy-Klein, C. Nguyen, C. Bordé and C. Chardonnet, Phys. Rev. Lett. **83** (1999) 1554.
43. H. Hollenstein, D. Luckhaus, J. Pochert, M. Quack and G. Seyfang, Angew. Chemie Intl. Ed. **36** (1997) 140.
44. R. Compton, unpublished work, cited in R. F. Service, Science **286** (1999) 1282.
45. J. Stohner, A. Beil, H. Hollenstein, O. Monti and M. Quack. In *37th IUPAC Congress and 27th GDCh Meeting, Berlin, Germany, August 14−19, 1999, Frontiers in Chemistry: Molecular Basis of the Life Sciences*, page 525. ISBN 3-924763-82-8; and M. Quack and J. Stohner, Phys. Rev. Lett. (2000) in press.
46. M. Quack and J. Stohner, in *SASP 2000 Proc. of the XIIth Symposium on Atomic and Surface Physics and related topics, January 30−February 5 (2000) eds. Davide Bassi and Paolo Tosi, Costa di Folgaria Universita di Trento (Italia) 2000.*
47. J. K. Laerdahl, P. Schwerdtfeger and H. M. Quiney, Phys. Rev. Lett. (2000) in press.
48. J. H. van't Hoff, Vorlesungen über theoretische und physikalische Chemie, Band 2, Vieweg, Braunschweig (1899); Die Lagerung der Atome im Raume, Vieweg, Braunschweig (1876); in B. M. Bazendijk (Ed.): La chimie dans l'espace, Rotterdam (1887).
49. P. J. Mohr and B. N. Taylor, J. Phys. Chem. Ref. Data **27** (1999).
50. M. Bouchiat and C. Bouchiat, J. Physique **35** (1974) 899.
51. C. Cohen-Tannoudji, B. Diu and F. Lalöe, *Quantum Mechanics. Vol. II*, John Wiley, New York (1977).
52. S. Fraga and G. Malli, *Many Electron Systems: Properties and Interactions*, W. B. Saunders Co., Philadelphia (1968). R. R. Ernst, G. Bodenhausen and A. Wokann, Principles of Nuclear Magnetic Resonance in One and Two Dimensions, Oxford, Clarendon Press.
53. H. Kiyonaga, K. Morihashi and O. Kikuchi, J. Chem. Phys. **108** (1998) 2041.
54. M. J. Frisch, G. W. Trucks, M. Head-Gordon, P. M. W. Gill, M. W. Wong, J. B. Foresman, B. G. Johnson, H. B. Schlegel, M. A. Robb, E. S. Replogle, R. Gomperts, J. L. Andres, K. Ragavachari, J. S. Binkley, C. Gonzales, R. L. Martin, D. J. Fox, D. J. Defrees, J. Baker, J. J. P. Stewart and J. A. Pople, Gaussian 94, Gaussian Inc., Pittsburgh PA (1994).
55. H. Ågren, O. Vahtras and B. Minaev, Adv. Quant. Chem. **27** (1996) 71.
56. T. Helgacker, H. Jensen, P. Joergensen, J. Olsen, K. Ruud, H. Ågren, T. Andersen, K. Bak, V. Bakken, O. Christiansen, P. Dahle, E. Dalskov, T. Enevoldsen, B. Fernan-

dez, H. Heiberg, H. Hettema, D. Jonsson, S. Kirpekar, R. Kobayashi, H. Koch, K. Mikkelsen, P. Norman, M. Packer, T. Saue, P. Taylor and O. Vahtras, DALTON, an Electronic Structure Program, release 1.0 (1997).
57. M. Quack, Annu. Rev. Phys. Chem. **41** (1990) 839.
58. E. B. Wilson Jr., J. C. Decius and P. C. Cross, *Molecular vibrations. The theory of infrared and Raman vibrational spectra.* McGraw-Hill Inc., New York (1955).
59. J. Murrell, S. Carter, S. Farantos, P. Huxley and A. Varandas, *Molecular Potential Energy Functions*, John Wiley, New York (1984).
60. M. Quack, Phil. Trans. R. Soc. Lond. **A332** (1990) 203.
61. M. Quack, J. Mol. Struct. **292** (1993) 171.
62. H. Hollenstein, R. Marquardt, M. Quack and M. A. Suhm, J. Chem. Phys. **101** (1994) 3588.
63. M. Quack and M. A. Suhm, Spectroscopy and quantum dynamics of hydrogen fluoride clusters, in J. Bowman and Z. Bačić, editors, *Advances in Molecular Vibration and Collision Dynamics, Vol. III Molecular Clusters*, pages 205−248, JAI Press (1998).
64. R. Marquardt and M. Quack, J. Chem. Phys. **109** (1998) 10628.
65. R. Meyer, J. Chem. Phys. **52** (1970) 2053.
66. D. Luckhaus and M. Quack, Chem. Phys. Lett. **190** (1992) 581.
67. A. Beil, H. Hollenstein, O. Monti, M. Quack and J. Stohner, J. Chem. Phys. in press (2000).
68. B. Char, K. Geddes, G. Gonnet, B. Leong, M. Monagan and S. Watt, *Maple V.* Waterloo Maple Software, Waterloo, Ontario (1990).
69. H. W. Kroto, *Molecular Rotation Spectra*, John Wiley, New York, first edition (1975).
70. D. Luckhaus and M. Quack, Mol. Phys. **68** (1989) 745.
71. A. Beil, D. Luckhaus, R. Marquardt and M. Quack, J. Chem. Soc. Faraday Discuss. **99** (1994) 96.
72. Y. Morino and K. Kuchitsu, J. Chem. Phys. **20** (1952) 1809.
73. M. Quack, Chapter 27 in "Femtosecond Chemistry" ed. by J. Manz and L. Woeste, Vch Publishers, Weinheim (1995) 781−817.
74. A. Schäfer, H. Horn and R. Ahlrichs, J. Chem. Phys. **97** (1992) 2571.